





[View Journal Online](#)  
[View Article Online](#)

## Exploring solvatochromism in Nile Blue 690 dye: Evaluating dipole moments across the ground and excited states

Darukaswamy Tulahalli Hirematada <sup>1,2</sup>, Mallikarjun Kalagouda Patil <sup>3</sup>,  
 Sanjeev Ramchandra Inamdar <sup>3</sup>, and Kotresh Mare Goudar <sup>1,\*</sup>

<sup>1</sup> Department of Physics, Faculty of Pure Science, Vijayanagara Sri Krishnadevaraya University, Ballari-583105, Karnataka, India

<sup>2</sup> Department of Physics, Faculty of Pure Science, Shri Shankar Anand Singh Government First Grade College, Hosapete-583201, Karnataka, India

<sup>3</sup> Department of Studies in Physics, Faculty of Pure Science, Laser Spectroscopic Laboratory, Karnatak University, Dharwad-580003, Karnataka, India

\* Corresponding author at: Department of Physics, Faculty of Pure Science, Vijayanagara Sri Krishnadevaraya University, Ballari-583105, Karnataka, India.  
 e-mail: [kotreshm26@vskub.ac.in](mailto:kotreshm26@vskub.ac.in) (K.M. Goudar).

### RESEARCH ARTICLE



doi 10.5155/eurjchem.15.2.178-185.2533

Received: 25 February 2024

Received in revised form: 13 April 2024

Accepted: 8 May 2024

Published online: 30 June 2024

Printed: 30 June 2024

### KEYWORDS

Nile blue 690  
 Dipole moment  
 Solvatochromism  
 Bakhshiev correlation technique  
 Lippert-Mataga correlation technique  
 Kawski-Chamma-Viallet correlation technique

### ABSTRACT

This study investigates the photophysical properties of Nile Blue 690 (NB-690) dye using spectroscopic techniques. Absorption and fluorescence spectroscopy were used to analyze NB-690, revealing pronounced bathochromic shifts in both absorption and fluorescence spectra, indicative of the  $\pi \rightarrow \pi^*$  transition. The study focuses on estimating ground- and excited-state dipole moments of NB-690 through solvatochromic shifts in absorption and fluorescence spectra. Various computational methods, including the Bilot-Kawski approach for ground state dipole moment computation, and the Reichardt correlation, the Bakhshiev, the Lippert-Mataga, and the Kawski-Chamma-Viallet methods for calculating the excited state dipole moment, were utilized. The results demonstrate excited-state dipole moment values of 6.922, 5.529, 5.529, 5.529, and 4.615 D, respectively, using the Lippert-Mataga, Bakhshiev, Kawski-Chamma-Viallet and solvent polarity correlation approaches. Significantly, the excited state dipole moment surpasses the ground state dipole moment, attributed to the significant  $\pi$ -electron density redistribution upon excitation. Intriguingly, both excited- and ground-state dipole moments align parallel to each other at a  $0^\circ$  angle. In general, these findings underscore the potential utility of NB-690 in optoelectronic applications, highlighting its responsiveness to environmental signals and providing valuable information for further exploration in the field.

Cite this: *Eur. J. Chem.* **2024**, *15*(2), 178-185

Journal website: [www.eurjchem.com](http://www.eurjchem.com)

### 1. Introduction

Nile blue dye, classified among oxazines, has intriguing photophysical characteristics, making it indispensable for various technological applications, particularly in optical and photonic devices [1-5]. Recent years have seen extensive research on the spectroscopic behavior of oxazine dyes [1-5]. In particular, the spectral attributes of Nile Blue and other oxazine dyes are highly sensitive to their surroundings, making them valuable in experimental applications and as molecular probes [6-14]. The molecular structure of Nile Blue encompasses an electron donor and an electron-withdrawing aromatic system, forming a push-pull conjugated system with two amino groups and a heterocyclic oxygen atom bridging the conjugation. Nile blue possesses hydrogen bond donor/acceptor groups, which facilitates potential hydrogen bonding in suitable solvents. Several studies have highlighted the photochemical and photophysical properties of these dyes, notably their pronounced solvatochromism that leads to substantial red shifts in absorption and emission maxima when transitioning from nonpolar to polar solvents [15-18].

This solvatochromic behavior stems from the substantial dipole moment change during electronic state transitions, which involves charge transfer between the diethylamino group (acting as an electron donor) and the aromatic acceptor system. Significant experimental studies have explored the dipole moments of various fluorescent dyes using methods such as the solvent shift method [19-24]. Furthermore, recent review articles provide valuable information on the effects of solvents on electronic spectra [25]. Spectroscopic methods based on dye absorption and emission offer qualitative information on intermolecular interactions, while solvatochromic methods provide a means of estimating singlet ground- and excited-state dipole moments, crucial for understanding electronic and geometric molecular structures in transient states [26-30].

Among the techniques for determining excited-state dipole moments, the solvatochromic method stands out as the most widely used, leveraging linear correlations between absorption and fluorescence maxima, wavenumbers, and solvent polarity functions derived from quantum mechanical theory. Lippert-Mataga, Bakhshiev and Kawski-Chamma-Viallet solvent polarity functions, using the dielectric constant ( $\epsilon$ ) and refractive index ( $n$ ) as empirical parameters, are particularly

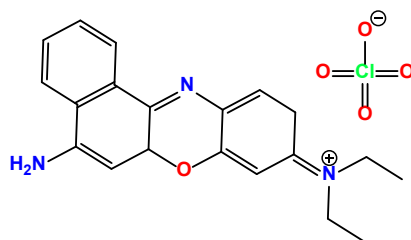


Figure 1. Molecular structure of the NB-690 laser dye.

common. These methods not only evaluate dipole moments but also quantify various solute–solvent interactions, leading to an improved understanding of spectral property correlations.

Despite extensive research on Nile blue optical properties, investigating ground-state and excited-state dipole moments in various liquid media remains a pertinent challenge. This study contributes by observing and comparing Nile Blue dipole moments across various solvents, shedding light on the nature and extent of solvent-solute interactions using multiparameter solvent polarity scales. Understanding these interactions is crucial for unraveling the excited state behavior of Nile Blue and gaining insights into solution chemistry.

Furthermore, understanding how solvents affect electronic transitions and dipole moments is crucial to unraveling the excited-state behavior of fluorophores and to gain insight into solution chemistry, a key aspect explored through solvatochromism. Nile blue, among various organic molecules, has served as a fluorescent probe for over a century, renowned for its characteristic shift in absorption and emission maxima toward red in polar environments. This shift indicates a stabilized charge separation in the excited state, rendering Nile Blue a valuable tool for monitoring solvent polarity-dependent events [31-36].

Nile blue also exhibits a higher affinity for cancerous cells compared to healthy cells and acts as an oxygen photosensitizer, potentially valuable in photodynamic therapy. However, Nile blue faces limitations in aqueous media because of its low solubility and quantum yield. To address these drawbacks, researchers have explored Nile blue derivatives with enhanced water solubility by introducing water-solubilizing substituents, reducing the aggregation tendency of flat lipophilic aromatic dyes such as Nile Blue and leading to improved quantum yields [37-43]. Despite advancements, such derivatives often lack comprehensive quantum yield data or detailed experimental synthesis procedures. This study aims to bridge this gap by focusing on Nile Blue-690 dye and investigating its photophysical properties through spectroscopic techniques, with potential applications including biochemical molecule detection and serving as biological stains, such as fluorescent lipid probes.

## 2. Experimental

The Nile Blue 690 (5-amino-9-(diethylamino) benzo(a) phenoxazin-7-ium perchlorate) used in this study was obtained from Exciton Chemical Co., USA and used without additional purification. The molecular structure of the NB 690 dye is illustrated in Figure 1. The spectroscopic grade solvents used in our research were purchased from Sigma-Aldrich.

Absorption spectra spanning the 300-700 nm range were acquired using a UV-vis absorption spectrophotometer (JASCO, Model V-670). Fluorescence spectra were recorded on a spectrofluorometer (Horiba, Fluoromax-4) with an integration time of 0.1 s/nm and 1 nm slit width. A quartz cuvette with a path length of 1 cm facilitated these measurements. The data obtained were meticulously analyzed using Origin 19 software.

## 3. Theory of solvatochromic shift methods

### 3.1. Bilot-Kawski approach

Bilot and Kawski [44] successfully derived a quantum mechanical relation using band shifts of absorption ( $\bar{\nu}_a$ ) and fluorescence ( $\bar{\nu}_f$ ) recorded in several solvents with varying permittivity ( $\epsilon$ ) and refractive index ( $n$ ). This quantum mechanical relation enables the representation of the maxima of absorption ( $\bar{\nu}_a$ ) and fluorescence ( $\bar{\nu}_f$ ) using the solvatochromism equations. These equations (Equations 1 and 2) provide a valuable tool for understanding the influence of solvent properties on the spectral behavior of the solute, allowing for the quantitative analysis of solvatochromic shifts in absorption and fluorescence.

$$\bar{\nu}_a - \bar{\nu}_f = m_{BK(1)} f(\epsilon, n) + constant \quad (1)$$

$$\bar{\nu}_a + \bar{\nu}_f = -m_{BK(2)} (f(\epsilon, n) + 2g(n)) + constant \quad (2)$$

where,  $f(\epsilon, n) = \frac{2n^2 + 1}{n^2 + 2} \left[ \frac{\epsilon - 1}{\epsilon + 2} - \frac{n^2 - 1}{n^2 + 2} \right]$  and

$g(n) = \frac{3}{2} \left[ \frac{n^4 - 1}{(n^2 + 2)^2} \right]$  are representing the solvent polarity

functions by means of the refractive index ( $n$ ); solvent permittivity ( $\epsilon$ ), the slopes obtained from Equations 1 and 2 are  $m_{BK(1)}$  and  $m_{BK(2)}$ , respectively, by Equations 3 and 4 given below.

$$m_{BK(1)} = \frac{2(\mu_e - \mu_g)^2}{hca^3} \quad (3)$$

$$m_{BK(2)} = \frac{2(\mu_e^2 - \mu_g^2)}{hca^3} \quad (4)$$

where  $a$ ,  $c$ , and  $h$  represent the radius of the Onsager cavity, the velocity of light, and Planck's constant, respectively.

Dipole moments in both ground ( $\mu_g$ ) and excited states ( $\mu_e$ ) are parallel if the solute molecule's symmetry is same during the electronic transition [45]. When this occurs,  $\mu_g$  and  $\mu_e$  are provided by the following Equations 5-7.

$$\mu_g = \frac{(m_{BK(2)} - m_{BK(1)})}{2} \sqrt{\frac{hca^3}{2m_{BK(1)}}} \quad (5)$$

$$\mu_e = \frac{(m_{BK(2)} + m_{BK(1)})}{2} \sqrt{\frac{hca^3}{2m_{BK(2)}}} \quad (6)$$

$$\text{and } \mu_e = \frac{(m_{BK(2)} + m_{BK(1)})}{(m_{BK(2)} - m_{BK(1)})} \mu_g \text{ for } m_{BK(2)} > m_{BK(1)} \quad (7)$$

Normally, the dipole moments ( $\mu_g$ ) as well as ( $\mu_e$ ), which are not parallel to each other [45], they make an angle  $\phi$  and Equation 8 can be used to approximate the angle  $\phi$  between them.

$$\cos \phi = \frac{1}{2\mu_g \mu_e} \left[ (\mu_e^2 + \mu_g^2) - \frac{m_{BK(1)}}{m_{BK(2)}} (\mu_e^2 - \mu_g^2) \right] \quad (8)$$

### 3.2. Lippert-Mataga, Bakhshiev, and Kawski-Chamma-Viallet approach

The solvatochromic techniques described by Lippert-Mataga [46,47], Bakhshiev [48], and Kawski-Chamma-Viallet [24] were represented as Equations 9-11, respectively, and can be employed to determine the experimentally measured dipole moments of the ground and singlet excited states. These equations provide a quantitative approach to relate solvatochromic shifts in absorption or fluorescence to changes in the dipole moment of the solute molecule. Using these solvatochromic techniques, the study aims to derive the dipole moments of both the ground and singlet excited states through experimental measurements.

$$\bar{\nu}_a - \bar{\nu}_f = m_{LM} F_{LM}(\varepsilon, n) + constant \quad (9)$$

$$\bar{\nu}_a - \bar{\nu}_f = m_B F_B(\varepsilon, n) + constant \quad (10)$$

$$\frac{\bar{\nu}_a + \bar{\nu}_f}{2} = -m_{KCV} F_{KCV}(\varepsilon, n) + constant \quad (11)$$

where

$$m_{LM} = \frac{2(\mu_e - \mu_g)^2}{hca^3} \quad (12)$$

$$m_B = \frac{2(\mu_e - \mu_g)^2}{hca^3} \quad (13)$$

$$m_{KCV} = \frac{2(\mu_e^2 - \mu_g^2)}{hca^3} \quad (14)$$

From the graphs of  $(\bar{\nu}_a - \bar{\nu}_f)$  versus  $F_{LM}$ ,  $F_B$ , and  $(\bar{\nu}_a + \bar{\nu}_f)/2$  versus  $F_{KCV}$  yields the slopes,  $m_B$ ,  $m_{LM}$ , and  $m_{KCV}$  are obtained respectively from Equations 12-14. Solvent polarity functions  $F_B$ ,  $F_{LM}$ , and  $F_{KCV}$  provided by Equations 15-17,

$$F_{LM}(\varepsilon, n) = \frac{\varepsilon - 1}{2\varepsilon + 1} - \frac{n^2 - 1}{2n^2 + 1} \quad (15)$$

$$F_B(\varepsilon, n) = \frac{2n^2 + 1}{n^2 + 2} \left[ \frac{\varepsilon - 1}{\varepsilon + 2} - \frac{n^2 - 1}{n^2 + 2} \right] \quad (16)$$

$$F_{KCV}(\varepsilon, n) = \left[ \frac{2n^2 + 1}{2(n^2 + 2)} \left( \frac{\varepsilon - 1}{\varepsilon + 2} - \frac{n^2 - 1}{n^2 + 2} \right) + \frac{3(n^4 - 1)}{2(n^2 + 2)^2} \right] \quad (17)$$

### 3.3. Investigational measured microscopic solvent polarity parameter approach

The experiential microscopic solvent polarity parameter scale  $E_T^N$ , proposed by Reichardt [29], has been found to correspond more accurately with the spectral shifts of molecules compared to methods based on bulk solvent polarity. There exists a relationship between the spectral shifts and the

microscopic solvent polarity parameter  $E_T^N$ , which is described by a specific relation given by Equations 18 and 19,

$$\bar{\nu}_a - \bar{\nu}_f = m_R E_T^N + constant \quad (18)$$

$$\text{where, } m_R = 11307.6 \left[ \left( \frac{\Delta\mu}{\Delta\mu_B} \right)^2 \left( \frac{a_B}{a} \right)^3 \right] \quad (19)$$

where, 'a' and 'a<sub>B</sub>' are the relative Onsager radii of the target molecule and the Betaine dye, respectively [49],  $\Delta\mu$  and  $\Delta\mu_B$  are the changes in the probe's dipole moment caused by excitation and that of the Betaine dye. The values for  $\Delta\mu_B$  and  $a_B$  have been reported 9D and 6.2 Å, respectively. The  $E_T^N$ , the normalized polarity function of the solvent suggested by Reichardt [29] is a dimensionless solvatochromic constraint defined based on the absorption wave number  $\bar{\nu}_a$  of a standard the Betaine dye in the solvent is given by Equation 20.

$$E_T^N = \frac{E_T(\text{Solvent}) - E_T(\text{TMS})}{E_T(\text{Water}) - E_T(\text{TMS})} = \frac{E_T(\text{Solvent}) - 30.7}{32.4} \quad (20)$$

By employing these values, Equation 21 may be used to determine the difference between the dipole moments of the ground and excited states;

$$\Delta\mu = \mu_e - \mu_g = \left[ \frac{m_R \times 81}{\left( \frac{6.2}{a} \right)^3 11307.6} \right]^{\frac{1}{2}} \quad (21)$$

where,  $m_R$  denotes the slope of polarity function of solvent  $E_T^N$  vs. Stokes shift. Tetramethylsilane (TMS) is commonly represented by the abbreviation TMS. In the context of the empirical solvent polarity parameter,  $E_T$  (solvent), the value ranges from 0 to 1.000, with TMS having a lower value, and water being highly polar with a value of 1.000. These variable values can be used in Equation 21 to estimate the change in dipole moments of the solute molecule.

The spectral properties of the dye were correlated with an index of solvent dipolarity/polarizability to measure a charge or dipole through nonspecific dielectric interactions ( $\pi^*$ ), indices of hydrogen bond donor (HBD) strength ( $\alpha$ ) and hydrogen bond acceptor (HBA) strength ( $\beta$ ) using the multiple linear regression method proposed by Kamlet *et al.* according to Equation 22 [50],

$$y = y_0 + a\alpha + b\beta + c\pi^* \quad (22)$$

where,  $y_0$  is the relevant spectroscopic property in the gas phase and  $y$  is the spectroscopic property of interest. The coefficients  $a$ ,  $b$ , and  $c$  represent the HBD, HBA, and nonspecific dielectric interactions of the solvents, respectively.

### 3.4. Determination of Onsager cavity radius

Using Equation 23 [33], the Onsager cavity radius 'a' of NB-690 dye was calculated and given by

$$a = \left[ \frac{3M}{4\pi\rho N_A} \right]^{\frac{1}{3}} \quad (23)$$

where,  $\rho$  is the density,  $M$  is the molecular weight of the molecule, and  $N_A$  is Avogadro's number.

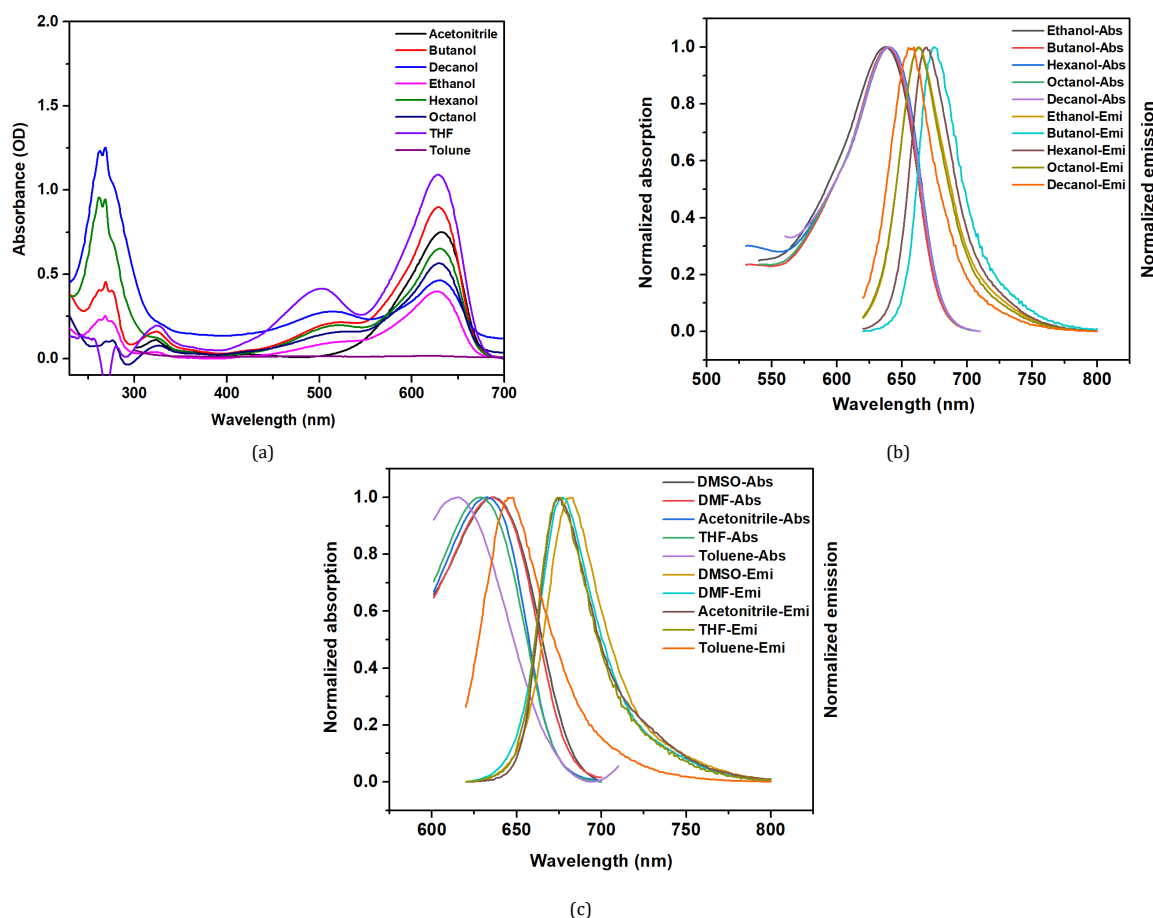


**Figure 2.** (a) Absorption spectra in different solvents, (b) Normalized absorption and emission in alcohols, and (c) Normalized absorption and emission in general solvents.

## 4. Results and discussion

### 4.1. Effect of solvents on absorbance and fluorescence spectra

The absorption spectrum of Nile Blue-690 typically shows peaks (Figure 2a) in two significant regions: one spanning from approximately 200 to 350 nm and another from 550 to 650 nm. The absorption peak observed in the 250 to 350 nm range can be attributed to  $\pi \rightarrow \pi^*$  transitions, where electrons are excited from the highest occupied molecular orbital (HOMO) to the lowest unoccupied molecular orbital (LUMO) within the dye molecule. This transition probably occurs due to the presence of conjugated  $\pi$ -systems within Nile Blue's chemical structure, facilitating electronic excitation. Conversely, the absorption peak in the 550 to 650 nm range may result from charge-transfer transitions, where electrons move between different regions of the molecule containing heteroatoms like nitrogen or oxygen. Factors such as solvent, environment, concentration, and molecular interactions can influence the exact positions and intensity of these absorption peaks. Therefore, the absorption spectrum of NB-690 reflects its complex electronic structure and its interaction with surrounding molecules, offering valuable information for various analytical and research endeavors.

The study involved examining the steady-state absorption and fluorescence spectra of the NB-690 dye across a spectrum of solvents with varying polarities. Figures 2b and 2c illustrate the typical absorption and fluorescence spectra observed in different alcohols and general solvents. Table 1 summarizes the absorption and emission maxima of NB-690 dye in these

solvents, quantifying the shifts in the spectra in terms of wavenumber ( $\text{cm}^{-1}$ ). The absorption maxima ranged from 614 to 638 nm, indicating a wavelength shift of 24 nm. Similarly, the fluorescence spectrum maxima ranged from 645 to 682 nm, demonstrating a shift of 37 nm compared to the absorption spectra.

In polar liquids (ethanol to decanol), the absorption maximum demonstrates a red shift from 627 to 630 nm, indicating a bathochromic shift. The behavior of Nile Blue organic dye in various solvents, particularly concerning the shifts in absorption and fluorescence maxima, can be elucidated through an understanding of solvent polarity and its interaction with dye molecules. In less polar solvents such as alcohols, the absorption maxima exhibit minimal shifts due to weak interactions with the dye's chromophore. In contrast, polar solvents induce larger shifts in absorption maxima as a result of stronger interactions that alter the energy levels of electronic transitions within the dye. Interestingly, while fluorescence maxima in alcohols show a large shift, indicative of the influence of the solvent's polarity on the excited-state energy levels of the dye, highly polar solvents may exhibit small shifts in fluorescence maxima. This phenomenon arises from the stabilizing effect of polar solvents on the excited state of the dye, mitigating significant changes in the wavelengths of fluorescence emission [51].

The Stokes shift demonstrates a range from 1084 to 698  $\text{cm}^{-1}$  as the solvent polarity changes, as indicated in Table 1. This variance in the Stokes shift signifies adjustments in the geometric configuration of the dye when it electronically transitions to an excited state.

**Table 1.** Spectral and photophysical parameters of the NB-690 dye in various solvent polarities.

Solvents	$\lambda_{\text{abs}}$ (nm)	$\lambda_{\text{emi}}$ (nm)	$\bar{\nu}_a$ $\text{cm}^{-1}$	$\bar{\nu}_f$ $\text{cm}^{-1}$	$\bar{\nu}_a + \bar{\nu}_f$ $\text{cm}^{-1}$	$\bar{\nu}_a - \bar{\nu}_f$ $\text{cm}^{-1}$	$(\bar{\nu}_a + \bar{\nu}_f)/2$ $\text{cm}^{-1}$
Toluene	614	645	16286	15503	31789	783	15895
THF	628	655	15923	14814	30737	1109	15369
Decanol	630	659	15873	15174	31047	699	15523
Octanol	630	663	15873	15082	30955	791	15477
Hexanol	630	669	15873	14947	30820	926	15410
Butanol	629	675	15898	14814	30712	1084	15356
Ethanol	627	662	15948	15105	31053	843	15527
Acetonitrile	632	674	15822	14836	30658	986	15329
DMF	636	677	15723	14771	30494	952	15247
DMSO	638	682	15673	14662	30335	1011	15168

**Table 2.** Solvent parameters and calculated values for solvent polarity functions.

Solvents	n	$\epsilon$	$\alpha$	$\pi^*$	$\beta$	$E_T^N$	$f(\epsilon, n)$	$g(n)$	$f(\epsilon, n) + 2g(n)$	$F_{LM}(\epsilon, n)$	$F_B(\epsilon, n)$	$F_{KCV}(\epsilon, n)$
Toluene	1.497	2.38	0.00	0.54	0.11	0.099	0.029	0.335	0.699	0.013	0.029	0.349
THF	1.407	7.58	0.00	0.58	0.55	0.207	0.549	0.277	1.102	0.210	0.549	0.551
Decanol	1.437	8.00	0.70	0.45	0.70	0.525	0.553	0.296	1.145	0.204	0.553	0.573
Octanol	1.429	9.80	0.77	0.40	0.81	0.537	0.613	0.291	1.196	0.222	0.614	0.598
Hexanol	1.418	13.00	0.80	0.40	0.80	0.559	0.686	0.284	1.254	0.243	0.686	0.627
Butanol	1.399	17.40	0.84	0.84	0.47	0.586	0.749	0.271	1.292	0.263	0.749	0.646
Ethanol	1.369	24.30	0.86	0.54	0.75	0.654	0.809	0.251	1.311	0.286	0.809	0.656
Acetonitrile	1.344	36.64	0.19	0.75	0.40	0.460	0.861	0.234	1.329	0.305	0.861	0.665
DMF	1.430	38.25	0.00	0.88	0.69	0.386	0.839	0.292	1.423	0.275	0.839	0.711
DMSO	1.359	47.24	0.08	0.71	0.76	0.355	0.877	0.244	1.366	0.304	0.877	0.683

The considerable alteration in the geometry of the ground state of the dye in response to varying solvent polarities implies a range of solute-solvent interactions in both the ground and singlet excited states. The influences of the solvent lead to notable adjustments in the shape, intensity, and position of the absorption and fluorescence bands, providing information on whether the solvent is more stabilized in the ground or excited state [52]. Table 2 presents Reichardt parameters, specific physical constants, and calculated functions, including  $F_{LM}(\epsilon, n)$ ,  $F_B(\epsilon, n)$ , and  $F_{KCV}(\epsilon, n)$ . In these scenarios, the energy in the excited state is more influenced than that in the ground state. Given the greater stability of NB-690 in the relaxed excited state ( $S_1$ ) compared to the ground state ( $S_0$ ), it is expected that the ground state dipole moment will be lower than the excited state dipole moment. Positive solvatochromism is often observed during excitation when the solute's dipole moment increases ( $\mu_g < \mu_e$ ) [33].

#### 4.2. Specific interactions of the solute and solvent

The specific interactions between the solute (NB-690 dye) and the solvent were analyzed using the Kamlet-Abboud-Taft (KAT) method. This approach involves examining various solvent parameters, including hydrogen bond donor ability ( $\alpha$ ), hydrogen bond acceptor ability ( $\beta$ ), and dipolarity/polarizability ( $\pi^*$ ), to understand their influence on the spectral properties of the solute. From the results obtained through multiple linear regression analysis ( $y_0 = 549$ ,  $a = 560$ ,  $b = 545$ , and  $c = 349$ ), along with the correlation coefficients, it was observed that the values of  $\alpha$  and  $\beta$  of the solvents have a more significant impact on the absorption maxima, fluorescence maxima, and the shifts of the spectral band compared to dipolarity/polarizability ( $\pi^*$ ). This suggests that specific interactions, particularly those involving hydrogen bonding, play a crucial role in determining the spectral behaviour of the NB-690 dye in different solvent environments.

The higher contribution of  $\alpha$  and  $\beta$  of the solvents implies that specific interactions dominate over nonspecific dielectric interactions in influencing the spectral properties of the NB-690 dye. Therefore, changes in the Stokes shifts, which reflect adjustments in the dye's geometric configuration upon electronic transition, are primarily controlled by the hydrogen bond donor and acceptor abilities of the solvent. In general, the analysis indicates that understanding the specific interactions between NB-690 dye and solvents, particularly hydrogen

bonding, is essential to elucidate the solvatochromic behavior observed in the study. This knowledge provides valuable information for tailoring solvent environments to control the spectral characteristics of the NB-690 dye for various applications.

#### 4.3. Estimation of ground and excited state dipole moment

In solvatochromism, the spectrum shift is predominantly influenced by solute-solvent interactions, particularly the dielectric constant and the refractive index of solvents. Shifts in a specific type of interaction are attributed to solvent n-donor,  $\pi$ -donor, hydrogen bonding, and other factors. The Bilot-Kawski correlations (Figure 3) use slopes ( $m_1$ ) and ( $m_2$ ) to determine both the ground state dipole moment and the excited state dipole moment using Equations 5 and 6, respectively. The solvatochromism technique, correlating Stokes shift and solvent polarity using Lippert-Mataga (Equation 9), Bakhshiev (Equation 10), Kawaski-Chamma-Viallet (Equation 11), and Reichardt correlation (Equation 18), is employed to estimate the ground state dipole moment and that of the excited state. The graphs of  $(\bar{\nu}_a - \bar{\nu}_f)$  vs.  $F_{LM}$ ,  $F_B$ , and  $(\bar{\nu}_a + \bar{\nu}_f)/2$  vs.  $F_{KCV}$  yield the slopes  $m_{LM}$ ,  $m_B$ , and  $m_{KCV}$  from Equations 12-14. Solvent polarity functions  $F_{LM}$ ,  $F_B$ , and  $F_{KCV}$  are provided by Equations 15-17. Table 3 presents the slopes ( $m_{LM}$ ,  $m_B$ ,  $m_{KCV}$ , and  $m_R$ ), correlation coefficients ( $R^2$ ), and the intercepts obtained by linear regression for these correlations. Some solvents deviate from linear fits (Figure 4), possibly due to close proximity interactions between the solute and the solvent.

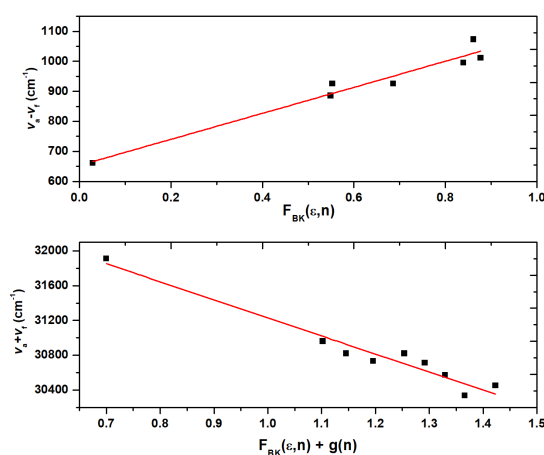
The empirical determination of the dipole moments is carried out using solvent correlation techniques. Ground and excited state dipole moments ( $\mu_g$  and  $\mu_e$ ) are estimated and presented in Table 4. The singlet excited-state dipole moment values are calculated from the slopes of Bakhshiev, Lippert-Mataga, Kawaski-Chamma-Viallet, and Reichardt correlations ( $m_B$ ,  $m_{LM}$ ,  $m_{KCV}$ , and  $m_R$ ). The Onsager cavity radii of the NB-690 dye were determined using Edwards' atomic increment approach. Furthermore, a remarkable consensus was observed among the calculated excited state dipole moments using various solvent correlation techniques, including the Reichardt microscopic solvent polarity correlation approach, Bakhshiev, Kawaski-Chamma-Viallet, and Lippert-Mataga methods. It should be noted that the Lippert-Mataga approach yields a larger  $\mu_e$  value compared to other methods due to the omission of polarizability when assessing the impact of the solute [52].

**Table 3.** Linear plot data for NB-690 obtained from different correlation methods.

Methods	Slope	Intercept	Correlation coefficient ( $R^2$ )	Number of data points
Bilot-Kawski	437 ( $m_1$ )	653	0.953	7
Bilot-Kawski	2074 ( $m_2$ )	33035	0.954	9
Lippert-Mataga	1295 ( $m_{LM}$ )	648	0.913	8
Bakhshiev	438 ( $m_B$ )	665	0.922	8
Kawski-Chamma-Viallet	2075 ( $m_{KCV}$ )	16650	0.965	9
Reichardt	637 ( $m_R$ )	614	0.974	8

**Table 4.** Ground- and excited-state dipole moments of NB-690 obtained from different correlation methods.

Excited state dipole moment, $\mu_e$ (D)				Ground state dipole moment, $\mu_g$ (D)	Change in dipole moment, $\Delta\mu$ (D)	Ratio of excited and ground state dipole moment	Angle between $\mu_e$ and $\mu_g$ ( $\Phi$ )	Onsager cavity radius 'a' (Å)		
Lippert-Mataga	Bakhshiev's	Kawski-Chamma-Viallet's	Bilot-Kawski	Solvent polarity parameter $E_T^N$	Bilot-Kawski	Solvatochromic equation	Solvent polarity equation $E_T^N$	$\mu_e/\mu_g$		
6.922	5.529	5.529	5.529	4.615	3.623	1.905	0.991	1.526	0	4.390

**Figure 3.** Linear plots of the Bilot and Kawski correlation for the NB-690 dye.

On the other hand, the dipole moments measured through the Bakhshiev, Kawski-Chamma-Viallet, and Solvatochromic method approaches demonstrate good agreement. The solvent polarity parameter typically results in a lower  $\mu_e$  value than the Bakhshiev, Kawski-Chamma-Viallet, and solvatochromic methods, possibly because these methods do not consider specific solute-solvent interactions such as hydrogen bonding, complex formation, and solvation molecular features, which are accounted for in the solvent polarity parameter method [53].

The ground state dipole moment ( $\mu_g$ ) is estimated using Equation 5 and was found to be 3.623 D, which is in good agreement with the theoretical value obtained in the literature using DFT calculations [53]. The ratio of the dipole moment in the excited state to that in the ground state is calculated to be 1.526. In particular, the positive dipole moment difference between the two electronic states ( $\Delta\mu > 0$ ) and the ratio greater than unity ( $\mu_e/\mu_g > 1$ ) suggest a significant charge distribution in the singlet excited state, indicative of involvement in the Intramolecular Charge Transfer (ICT) process. The higher dipole moment value in the singlet excited state than in the ground state implies a more pronounced polarization of the molecule in the former state.

The relatively small difference between the ground and excited-state dipole moments of Nile Blue dye can be attributed to several factors related to its molecular structure and electronic configuration. This includes the likely symmetrical molecular structure or minimal structural changes upon excitation, as well as the electronic configuration that does not undergo significant rearrangements upon excitation, leading to a stable dipole moment. Additionally, if the dye contains

conjugated systems, such as alternating single and double bonds, the distribution of electron density across the molecule may remain relatively constant between the ground and excited states. Moreover, the solvent environment and molecular interactions also play a role in influencing the dipole moment difference, with factors like solvent polarity, nearby molecules, and specific molecular configurations contributing to the observed dipole moment values. This underscores the strong solute-solvent interaction in each molecule, which results in a broad charge distribution in the excited singlet state [54,55].

## 5. Conclusions

In conclusion, our extensive investigation of Nile Blue-690 dye has provided significant insight into its behavior under varying solvent conditions. Through rigorous experimental techniques and the application of solvatochromic shift methods, we have elucidated key aspects of the molecule's physico-chemical properties. Our findings indicate a distinct disparity between the ground and excited-state dipole moments of NB-690. Specifically, the excited-state dipole moment consistently exceeds its ground-state counterpart across multiple correlation techniques. For instance, employing Bilot-Kawski's approach, the ground-state dipole moment is estimated at 3.623 Debye (D), while the excited-state dipole moment, determined through Lippert-Mataga, Bakhshiev, Kawski-Chamma-Viallet, and Reichardt correlations, consistently surpasses this value. These observations carry significant implications, particularly in the context of optoelectronics.

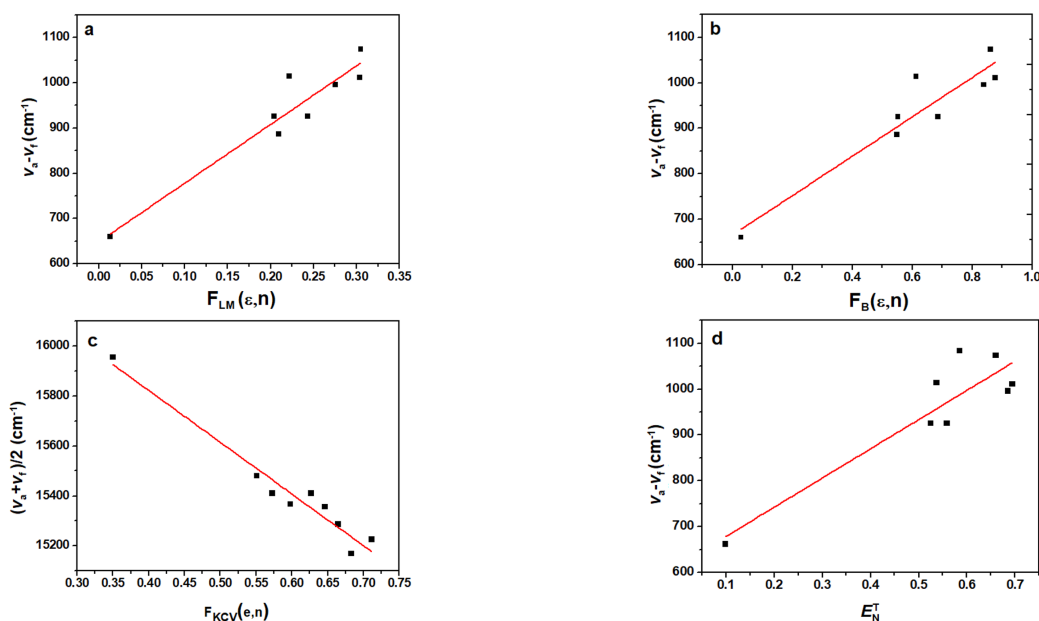


Figure 4. Linear plots of (a) Lippert-Mataga, (b) Baksheiv, (c) Kawaski-Chamma-Viallet, and (d) Reichard correlation for NB-690 dye.

The increased sensitivity of NB-690 to solvent polarity variations suggests its potential utility in optoelectronic applications where environmental responsiveness is crucial. Furthermore, our findings underscore the need for further theoretical refinement, as discrepancies between experimental and theoretical values necessitate deeper investigation and model enhancement. In summary, our investigation has contributed valuable information on the solvatochromic behavior of the Nile Blue-690 dye. Moving forward, these findings pave the way for continued exploration and exploitation of the unique properties of NB-690 in diverse scientific and technological endeavors.

### Acknowledgements

The authors acknowledge the University Scientific Instrument Centre of Karnataka University which provided a UV-Vis NIR Spectrophotometer and a Laser Spectroscopic Laboratory, Department of Physics, Karnataka University, Dharwad, which provided a spectrofluorometer with which photoluminescence spectra were obtained for the research work.

### Disclosure statement

Conflict of interest: The authors declare that they have no conflict of interest. Ethical approval: All ethical guidelines have been adhered to. Sample availability: Samples of the compounds are available from the author.


### CRedit authorship contribution statement

Conceptualization: Kotresh Mare Goudar, Darukaswamy Tulahalli Hirematada; Methodology: Darukaswamy Tulahalli Hirematada, Mallikarjun Kalagouda Patil; Validation: Mallikarjun Kalagouda Patil; Formal Analysis: Darukaswamy Tulahalli Hirematada, Mallikarjun Kalagouda Patil; Investigation: Darukaswamy Tulahalli Hirematada, Mallikarjun Kalagouda Patil, Sanjeev Ramchandra Inamdar, Kotresh Mare Goudar; Resources: Sanjeev Ramchandra Inamdar, Kotresh Mare Goudar; Data Curation: Darukaswamy Tulahalli Hirematada, Mallikarjun Kalagouda Patil; Writing - Original Draft: Darukaswamy Tulahalli Hirematada; Writing-Review and Editing: Darukaswamy Tulahalli Hirematada, Mallikarjun Kalagouda Patil, Sanjeev Ramchandra Inamdar, Kotresh Mare Goudar; Visualization: Darukaswamy Tulahalli Hirematada.


### ORCID and Email

Darukaswamy Tulahalli Hirematada

 [darukaswamy@gmail.com](mailto:darukaswamy@gmail.com)


 <https://orcid.org/0009-0009-5984-8798>

Mallikarjun Kalagouda Patil

 [mkpatilphy@gmail.com](mailto:mkpatilphy@gmail.com)

 <https://orcid.org/0000-0001-7126-9486>

Sanjeev Ramchandra Inamdar

 [him\\_lax3@yahoo.com](mailto:him_lax3@yahoo.com)

 <https://orcid.org/0000-0003-3398-4897>

Kotresh Mare Goudar

 [kotreshm26@gmail.com](mailto:kotreshm26@gmail.com)

 [kotreshm26@vskub.ac.in](mailto:kotreshm26@vskub.ac.in)

 <https://orcid.org/0000-0001-8738-2221>

### References

- Jose, J.; Burgess, K. Benzophenoxazine-based fluorescent dyes for labeling biomolecules. *Tetrahedron* **2006**, *62*, 11021–11037.
- Ghoneim, N. Photophysics of Nile red in solution. *Spectrochim. Acta A Mol. Biomol. Spectrosc.* **2000**, *56*, 1003–1010.
- Ghanadzadeh, A.; Zeini, A.; Kashef, A. Environment effect on the electronic absorption spectra of crystal violet. *J. Mol. Liq.* **2007**, *133*, 61–67.
- Ghanadzadeh Gilani, A.; Moghadam, M.; Zakerhamidi, M. S. Solvatochromism of Nile red in anisotropic media. *Dyes Pigm.* **2012**, *92*, 1052–1057.
- Blanchard, G. J. Ultrafast stimulated emission spectroscopy. In *Topics in Fluorescence Spectroscopy*; Springer US: Boston, MA, 2002; pp. 253–303.
- Kubinyi, M.; Grofcsik, A.; Pápai, I.; Jeremy Jones, W. Rotational reorientation dynamics of nile blue A and oxazine 720 in protic solvents. *Chem. Phys.* **2003**, *286*, 81–96.
- Grofcsik, A.; Kubinyi, M.; Ruzsinszky, A.; Veszprémi, T.; Jones, W. J. Quantum chemical studies on excited state intermolecular proton transfer of oxazine dyes. *J. Mol. Struct.* **2000**, *555*, 15–19.
- Simon, J. D.; Thompson, P. A. Spectroscopy and rotational dynamics of oxazine 725 in alcohols: A test of dielectric friction theories. *J. Chem. Phys.* **1990**, *92*, 2891–2896.
- Blanchard, G. J. A study of the state-dependent reorientation dynamics of oxazine 725 in primary normal aliphatic alcohols. *J. Phys. Chem.* **1988**, *92*, 6303–6307.
- Sackett, D. L.; Wolff, J. Nile red as a polarity-sensitive fluorescent probe of hydrophobic protein surfaces. *Anal. Biochem.* **1987**, *167*, 228–234.
- Fleming, S.; Mills, A.; Tuttle, T. Predicting the UV-vis spectra of oxazine dyes. *Beilstein J. Org. Chem.* **2011**, *7*, 432–441.
- Sackett, D. L.; Knutson, J. R.; Wolff, J. Hydrophobic surfaces of tubulin probed by time-resolved and steady-state fluorescence of nile red. *J. Biol. Chem.* **1990**, *265*, 14899–14906.
- Hejazi, M. S.; Raouf, J.-B.; Ojani, R.; Golabi, S. M.; Asl, E. H. Brilliant cresyl blue as electroactive indicator in electrochemical DNA oligonucleotide sensors. *Bioelectrochemistry* **2010**, *78*, 141–146.

- [14]. Ensafi, A. A.; Amini, M. A highly selective optical sensor for catalytic determination of ultra-trace amounts of nitrite in water and foods based on brilliant cresyl blue as a sensing reagent. *Sens. Actuators B Chem.* **2010**, *147*, 61–66.
- [15]. Peng, J.-J.; Liu, S.-P.; Wang, L.; He, Y.-Q. Studying the interaction between CdTe quantum dots and Nile blue by absorption, fluorescence and resonance Rayleigh scattering spectra. *Spectrochim. Acta A Mol. Biomol. Spectrosc.* **2010**, *75*, 1571–1576.
- [16]. Jose, J.; Ueno, Y.; Burgess, K. Water-soluble Nile Blue derivatives: Syntheses and photophysical properties. *Chem. Eur. J.* **2009**, *15*, 418–423.
- [17]. Zheng, H.; Chen, X.-L.; Zhu, C.-Q.; Li, D.-H.; Chen, Q.-Y.; Xu, J.-G. Brilliant cresyl blue as a new red region fluorescent probe for determination of nucleic acids. *Microchem. J.* **2000**, *64*, 263–269.
- [18]. Gilani, A. G.; Moghadam, M.; Zakerhamidi, M. S. Dimeric spectra analysis in Microsoft Excel: A comparative study. *Comput. Methods Programs Biomed.* **2011**, *104*, 175–181.
- [19]. Mannekutla, J. R.; Mulimani, B. G.; Inamdar, S. R. Solvent effect on absorption and fluorescence spectra of coumarin laser dyes: Evaluation of ground and excited state dipole moments. *Spectrochim. Acta A Mol. Biomol. Spectrosc.* **2008**, *69*, 419–426.
- [20]. Tipperudrappa, J.; Biradar, D. S.; Manohara, S. R.; Hanagodimath, S. M.; Inamdar, S. R.; Manekutla, R. J. Solvent effects on the absorption and fluorescence spectra of some laser dyes: Estimation of ground and excited-state dipole moments. *Spectrochim. Acta A Mol. Biomol. Spectrosc.* **2008**, *69*, 991–997.
- [21]. Rautela, R.; Joshi, N. K.; Joshi, H. C.; Tewari, N.; Pant, S. Solvatochromic study of 2-hydroxy-4-methylquinoline for the determination of dipole moments and solute-solvent interactions. *J. Mol. Liq.* **2010**, *154*, 47–51.
- [22]. Tewari, N.; Joshi, N. K.; Rautela, R.; Gahlaut, R.; Joshi, H. C.; Pant, S. On the ground and excited state dipole moments of dansylamide from solvatochromic shifts of absorption and fluorescence spectra. *J. Mol. Liq.* **2011**, *160*, 150–153.
- [23]. Kanya, R.; Ohshima, Y. Determination of dipole moment change on the electronic excitation of isolated Coumarin 153 by pendular-state spectroscopy. *Chem. Phys. Lett.* **2003**, *370*, 211–217.
- [24]. Kawski, A. On the estimation of excited-state dipole moments from solvatochromic shifts of absorption and fluorescence spectra. *Z. Naturforsch. A* **2002**, *57*, 255–262.
- [25]. Homocianu, M.; Airinei, A.; Dorohoi, D. O.; Olariu, I.; Fifere, N. Solvatochromic effects in the UV/vis absorption spectra of some pyridazinium ylides. *Spectrochim. Acta A Mol. Biomol. Spectrosc.* **2011**, *82*, 355–359.
- [26]. Kawski, A.; Kukliński, B.; Bojarski, P. Excited state dipole moments of 4-(dimethylamino)benzaldehyde. *Chem. Phys. Lett.* **2007**, *448*, 208–212.
- [27]. Raikar, U. S.; Renuka, C. G.; Nadaf, Y. F.; Mulimani, B. G.; Karguppikar, A. M.; Soudagar, M. K. Solvent effects on the absorption and fluorescence spectra of coumarins 6 and 7 molecules: Determination of ground and excited state dipole moment. *Spectrochim. Acta A Mol. Biomol. Spectrosc.* **2006**, *65*, 673–677.
- [28]. Biradar, D. S.; Siddlingeshwar, B.; Hanagodimath, S. M. Estimation of ground and excited state dipole moments of some laser dyes. *J. Mol. Struct.* **2008**, *875*, 108–112.
- [29]. Reichardt, C. Solvatochromic dyes as solvent polarity indicators. *Chem. Rev.* **1994**, *94*, 2319–2358.
- [30]. Ghanadzadeh Gilani, A.; Hosseini, S. E.; Moghadam, M.; Alizadeh, E. Excited state electric dipole moment of Nile blue and brilliant cresyl blue: A comparative study. *Spectrochim. Acta A Mol. Biomol. Spectrosc.* **2012**, *89*, 231–237.
- [31]. Martinez, V.; Henary, M. Nile red and Nile blue: Applications and syntheses of structural analogues. *Chemistry* **2016**, *22*, 13764–13782.
- [32]. Arslan, H.; Mansuroglu, D. S.; VanDerveer, D.; Binzet, G. The molecular structure and vibrational spectra of N-(2,2-diphenylacetyl)-N'-(naphthalen-1yl)-thiourea by Hartree-Fock and density functional methods. *Spectrochim. Acta A Mol. Biomol. Spectrosc.* **2009**, *72*, 561–571.
- [33]. Lombardi, J. R. Correlation between structure and dipole moments in the excited states of substituted benzenes. *J. Am. Chem. Soc.* **1970**, *92*, 1831–1833.
- [34]. Lee, S. H.; Suh, J. K.; Li, M. Determination of bovine serum albumin by its enhancement effect of Nile blue fluorescence. *Bull. Korean Chem. Soc.* **2003**, *24*, 45–48.
- [35]. Das, K.; Jain, B.; Patel, H. S. Nile Blue in Triton-X 100/benzene-hexane reverse micelles: a fluorescence spectroscopic study. *Spectrochim. Acta A Mol. Biomol. Spectrosc.* **2004**, *60*, 2059–2064.
- [36]. Krihak, M.; Murtagh, M. T.; Shahriari, M. R. Spectroscopic Study of the Effects of Various Solvents and Sol-Gel Hosts on the Chemical and Photochemical Properties of Thionin and Nile Blue A. *J. Solgel Sci. Technol.* **1997**, *10*, 153–163.
- [37]. Maliwal, B. P.; Kuśba, J.; Lakowicz, J. R. Fluorescence energy transfer in one dimension: Frequency-domain fluorescence study of DNA-fluorophore complexes. *Biopolymers* **1995**, *35*, 245–255.
- [38]. Lakowicz, J. R.; Piszczek, G.; Kang, J. S. On the possibility of long-wavelength long-lifetime high-quantum-yield luminophores. *Anal. Biochem.* **2001**, *288*, 62–75.
- [39]. Nikas, D. C.; Foley, J. W.; Black, P. M. Fluorescent imaging in a glioma model in vivo. *Lasers Surg. Med.* **2001**, *29*, 11–17.
- [40]. Lin, C. E.; Shulok, J. R.; Wong, Y. K.; Schanbacher, C. F.; Cincotta, L.; Foley, J. W. Photosensitization, Uptake, and Retention of Phenoxazine Nile Blue Derivatives in Human Bladder Carcinoma Cells. *Cancer Res* **1991**, *51* (4), 1109–1116 <https://aacrjournals.org/cancerres/article/51/4/1109/497497/Photosensitization-Uptake-and-Retention-of>.
- [41]. Lin, C.-W.; Shulok, J. R. Enhancement of Nile blue derivative-induced photocytotoxicity by nigericin and low cytoplasmic pH. *Photochem. Photobiol.* **1994**, *60*, 143–146.
- [42]. Pihlasalo, S.; Engbert, A.; Martikkala, E.; Ylander, P.; Hänninen, P.; Härmä, H. Nonspecific particle-based method with two-photon excitation detection for sensitive protein quantification and cell counting. *Anal. Chem.* **2013**, *85*, 2689–2696.
- [43]. Nadaf, Y. F.; Mulimani, B. G.; Gopal, M.; Inamdar, S. R. Ground and excited state dipole moments of some exalite UV laser dyes from solvatochromic method using solvent polarity parameters. *Theochem.* **2004**, *678*, 177–181.
- [44]. Bilot, L.; Kawski, A. Zur Theorie des Einflusses von Lösungsmitteln auf die Elektronenspektren der Moleküle. *Z. Naturforsch. A* **1962**, *17*, 621–627.
- [45]. Rabek, J. F. *Progress in Photochemistry and Photophysics, Volume V*; CRC Press: Boca Raton, FL, 1992.
- [46]. Lippert, E. Dipolmoment und Elektronenstruktur von angeregten Molekülen. *Z. Naturforsch. A* **1955**, *10*, 541–545.
- [47]. Mataga, N.; Kaifu, Y.; Koizumi, M. Solvent effects upon fluorescence spectra and the dipole moments of excited molecules. *Bull. Chem. Soc. Jpn.* **1956**, *29*, 465–470.
- [48]. Bakshiev, N. G. Universal molecular interactions and their effect on the position of the electronic spectra of molecules in two-component solutions. *Opt. Spectrosc.* **1961**, *10*, 379–384.
- [49]. Rauf, M. A.; Graham, J. P.; Bukallah, S. B.; Al-Saedi, M. A. S. Solvatochromic behavior on the absorption and fluorescence spectra of Rose Bengal dye in various solvents. *Spectrochim. Acta A Mol. Biomol. Spectrosc.* **2009**, *72*, 133–137.
- [50]. Lee, J.-M.; Ruckes, S.; Prausnitz, J. M. Solvent polarities and Kamlet-Taft parameters for ionic liquids containing a pyridinium cation. *J. Phys. Chem. B* **2008**, *112*, 1473–1476.
- [51]. Edward, J. T. Molecular volumes and the Stokes-Einstein equation. *J. Chem. Educ.* **1970**, *47*, 261.
- [52]. Najare, M. S.; Patil, M. K.; Mantur, S.; Nadaf, A. A.; Inamdar, S. R.; Khazi, I. A. M. Highly conjugated D- $\pi$ -A- $\pi$ -D form of novel benzo[b]thiophene substituted 1,3,4-oxadiazole derivatives; Thermal, optical properties, solvatochromism and DFT studies. *J. Mol. Liq.* **2018**, *272*, 507–519.
- [53]. Kostjukov, V.; Leontieva, S.; Savchenko, E.; Rybakova, K.; Voronin, D. Photoexcitation of Nile blue dye in aqueous solution: Td-dft study. *Russian Journal of Biological Physics and Chemistry* **2022**, *7*, 209–221.
- [54]. Mehata, M. S.; Singh, A. K.; Sinha, R. K. Experimental and theoretical study of hydroxyquinolines: hydroxyl group position dependent dipole moment and charge-separation in the photoexcited state leading to fluorescence. *Methods Appl. Fluoresc.* **2016**, *4*, 045004.
- [55]. Suppan, P. Excited-state dipole moments from absorption/fluorescence solvatochromic ratios. *Chem. Phys. Lett.* **1983**, *94*, 272–275.



Copyright © 2024 by Authors. This work is published and licensed by Atlanta Publishing House LLC, Atlanta, GA, USA. The full terms of this license are available at <https://www.eurjchem.com/index.php/eurjchem/terms> and incorporate the Creative Commons Attribution-Non Commercial (CC BY-NC) (International, v4.0) License (<http://creativecommons.org/licenses/by-nc/4.0>). By accessing the work, you hereby accept the Terms. This is an open access article distributed under the terms and conditions of the CC BY-NC License, which permits unrestricted non-commercial use, distribution, and reproduction in any medium, provided the original work is properly cited without any further permission from Atlanta Publishing House LLC (European Journal of Chemistry). No use, distribution, or reproduction is permitted which does not comply with these terms. Permissions for commercial use of this work beyond the scope of the License (<https://www.eurjchem.com/index.php/eurjchem/terms>) are administered by Atlanta Publishing House LLC (European Journal of Chemistry).